Headline Articles

Triangular Platinum(II) Cluster Complexes and Cluster Core Transformation from Square-Planar to Triangular Type

Tadashi Yamaguchi,* Nozomu Nishimura, Ken-ichi Shirakura, and Tasuku Ito*

Department of Chemistry, Graduate School of Science, Tohoku University, Sendai 980-8578

(Received December 24, 1999)

Reactions of $[Pt^{II}_4(\mu\text{-}CH_3COO)_8]$ (**1**) with dioximes or with *N,N'*-dimethylethylenediamine induced a cluster core transformation from a square planar to a triangular type to afford Pt^{II}_3 clusters. Three of these clusters have been characterized by X-ray analyses. The structure of the Pt^{II}_3 cluster core is an approximate or regular isosceles triangle, two equidistant edges (2.51—2.56 Å) being somewhat shorter than the other (2.59—2.61 Å). The cluster core transformation proceeds through the substitution of the in-plane acetate ligands in **1** by incoming ligands followed by the removal of one Pt atom from the tetranuclear cluster core. An intermediate of the cluster core transformation, $[\{Pt_4(CH_3COO)_4(dmgH)_2(dmgH_2)\}_2(\mu\text{-}dmgH_2)]$, was structurally characterized. It is a dimer of tetranuclear Pt(II) complex and consists of a triangular cluster unit and a mononuclear unit with square planar geometry. EHMO study and large $^1J_{Pt-Pt}$ values of ca. 8000 Hz suggest the stability of the triangular Pt^{II}_3 cluster core and the existence of strong Pt–Pt bonds. Ligands in the Pt^{II}_3 cluster plane are labilized by trans effect of Pt–Pt bonds, although intramolecular hydrogen bonds reduce the lability. On the other hand, out-of-plane acetate ligands are substitution inert.

Platinum cluster complexes with Pt–Pt bonds are known for various oxidation states. Many of them are low-valent platinum clusters.[1—3] Tervalent platinum also forms dimeric cluster complexes[4,5] or compounds such as platinum blue in a Pt(II)/Pt(III) mixed valence state.[6] Divalent platinum clusters, however, had been limited to the octaacetato complex $[Pt^{II}_4(\mu\text{-}CH_3COO)_8]$ (**1**),[7] until we reported its derivatives.[5,8—11] Previously we reported that the acetate ligands in **1** which are in the plane of the square-planar Pt cluster core are labile, whereas the out-of-plane ligands are inert to substitution, and that many derivatives of **1** can be prepared via the substitution reaction.[8] We found also that **1** acts as an effective catalyst for hydrolysis of acetonitrile.[11,12] It has been shown that the regioselective substitution reactivity and the catalytic activity characteristic of **1** result from the Pt–Pt bonds in the cluster core which labilize coordination sites trans to the intermetallic bonds.[8,11] In the course of the study on the reactivities of **1**, we found that, upon reaction with some dioximes or with *N,N'*-dimethylethylenediamine (Me_2en), **1** undergoes a cluster core transformation to afford new Pt(II) cluster complexes having a novel triangular core. Some of the resulting Pt^{II}_3 complexes undergo in-plane ligand substitution to afford new derivatives with the same Pt^{II}_3 cluster core. In this paper, we report chemistries of novel Pt(II) triangular clusters, syntheses, structures, reactivities, and the mechanism of the cluster core transformation from a square-planar to a triangular type. In this study, dimethylglyoxime ($dmgH_2$), cyclohexanedione dioxime ($cdoH_2$), diphenylglyoxime ($dpgH_2$), benzoquinone dioxime ($bqdH_2$), were used as a dioxime ligand (Chart 1). Five Pt^{II}_3 clusters were isolated and characterized: $[Pt_3(CH_3COO)_4(dmgH)_2(dmgH_2)]$ (**2**), $[Pt_3(CH_3COO)_4(cdoH)_2(cdoH_2)]$ (**3**), $[Pt_3(CH_3COO)_4(dpgH)_2(dpgH_2)]$ (**4**), $[Pt_3(CH_3COO)_4(bqdH)_2(bqdH_2)]$ (**5**), and $[Pt_3(CH_3COO)_4(Me_2en)_3]^{2+}$ (**6**).[13] Preliminary results on **2** and **3** have been published.[14]

Results and Discussion

Syntheses of Trinuclear Platinum(II) Clusters. When tetranuclear cluster **1** is allowed to react with an excess of dimethylglyoxime ($dmgH_2$), **1** undergoes the cluster core transformation from a square-planar to a triangular type to give $[Pt_3(CH_3COO)_4(dmgH)_2(dmgH_2)]$ (**2**) (Eq. 1).[15]

$$[Pt_4(CH_3COO)_8] + 5\ dmgH_2 \longrightarrow [Pt_3(CH_3COO)_4(dmgH)_2(dmgH_2)] + [Pt(dmgH)_2] \downarrow + 4\ CH_3COOH \quad (1)$$

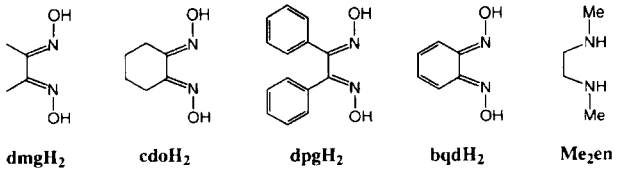

Chart 1.

Other dioximes such as cyclohexanedione dioxime ($cdoH_2$), diphenylglyoxime ($dpgH_2$), and benzoquinone dioxime ($bqdH_2$), undergo a similar reaction with **1** to afford trinuclear platinum(II) clusters $[Pt_3(CH_3COO)_4(dioxH)_2(dioxH_2)]$ ($dioxH_2$ = $cdoH_2$ (**3**), $dpgH_2$ (**4**), $bqdH_2$ (**5**)).[13,16]

Conditions for completion of the reaction depend strongly on the nature of the dioxime ligand. For example, the reaction with $dmgH_2$ requires that one reflux the reaction mixture for several hours, whereas that with $bqdH_2$ is completed in several minutes at room temperature. Required conditions for completion of the reaction are harder in the order: $dmgH_2 > cdoH_2 \approx dpgH_2 > bqdH_2$. The donating ability ($pK_a$) of the dioxime ligand does not account for the trend.[17] It appears that the trend corresponds to the rigidity of the dioxime ligand.

The same type of the cluster core transformation occurred also when a bulky bidentate chelate ligand other than dioximes such as *N*,*N*′-dimethylethylenediamine (Me_2en) was used (Eq. 2).

$$[Pt_4(CH_3COO)_8] + 5\,Me_2en \longrightarrow [Pt_3(CH_3COO)_4(Me_2en)_3]^{2+} + [Pt(Me_2en)_2]^{2+} + 4\,CH_3COO^- \quad (2)$$

Attempts to use either more bulky *N*,*N*,*N*′,*N*′-tetramethylethylenediamine (Me_4en) or unsubstituted ethylenediamine (en) were unsuccessful. Me_4en did not react with **1** at all, probably because of steric reasons. On the other hand, reaction of **1** with ethylenediamine afforded exclusively $[Pt_4(CH_3COO)_4(en)_4]^{4+}$, a substitution product of **1**, as reported previously.[9] These facts suggest that stereochemistry of entering ligand is concerned with the cluster core transformation. Note that $[Pt_3(CH_3COO)_4(Me_2en)_3]^{2+}$ (**6**) is dicationic, whereas dioxime ligand complexes **2**—**5** are neutral.

Structures of Triangular Platinum(II) Clusters. Structures of $[Pt_3(CH_3COO)_4(dmgH)_2(dmgH_2)]\cdot CH_2Cl_2$ (**2**·CH_2Cl_2), $[Pt_3(CH_3COO)_4(cdoH)_2(cdoH_2)]\cdot 2CH_3CN$ (**3**·$2CH_3CN$), and $[Pt_3(CH_3COO)_4(Me_2en)_3](ClO_4)_2\cdot 2NaClO_4$ (**6**$(ClO_4)_2\cdot 2NaClO_4$) have been determined by X-ray analyses. Crystallographic and structural determination data are listed in Table 1. Selected bond distances and angles are given in Table 2. Figure 1 shows ORTEP drawings of dmg complex **2** and Me_2en complex **6**. The overall structures of these clusters are very similar to each other.[16] The cluster core comprised of three Pt atoms is an approximate or regular isosceles triangle in all the clusters. Two equidistant edges of the isosceles triangle (2.51—2.56 Å) are somewhat shorter than the other (2.59—2.61 Å). The difference is larger in dioxime clusters than in Me_2en cluster, but all the distances indicate the existence of Pt–Pt bonds. As compared with Pt–Pt bond distance of 2.50 Å in tetranuclear cluster **1**,[7] those in the present Pt_3 clusters are slightly longer. Especially, the Pt–Pt bond of the longer edge (2.59—2.61 Å) lengthens definitely compared to those in tetranuclear platinum(II) complexes thus far structurally characterized.[7—11,18] The coordination geometry around each Pt is a distorted octahedron if the Pt–Pt bond is included. All the clusters have four acetate ligands at coordination sites perpendicular to the cluster plane. Two act as bridging ligands between Pt atoms at both ends of two equidistant edges of the triangle (Pt1–Pt2 and Pt2–Pt3), and are disposed toward opposite sides with respect to the cluster plane. The remaining two acetates are coordinated in a unidentate fashion to Pt atoms at both ends of the long edge. No acetate bridge exists over the long edge. Four acetates are arranged in an up-down-up-down sequence

Table 1. Crystallographic Data for **2**·CH_2Cl_2, **3**·$2CH_3CN$, **6**$(ClO_4)\cdot 2Na(ClO_4)$, and **8**·$8CH_2Cl_2$

	2·CH_2Cl_2	**3**·$2CH_3CN$	**6**$(ClO_4)_2\cdot 2NaClO_4$	**8**·$8CH_2Cl_2$
Empirical formula	$Pt_3C_{21}H_{36}O_{14}N_6Cl_2$	$Pt_3C_{30}H_{46}O_{14}N_8$	$Pt_3C_{20}H_{42}O_{24}N_6Cl_4Na_2$	$Pt_8Cl_{16}O_{30}N_{14}C_{52}H_{82}$
Formula weight	1250.71	1328.01	1523.64	3511.26
Space group	$P\bar{1}$ (#2)	$P\bar{1}$ (#2)	$C2/c$ (#15)	$P\bar{1}$ (#2)
a/Å	12.334(2)	12.376(3)	21.458(8)	13.1800(8)
b/Å	16.053(3)	16.898(4)	12.501(7)	14.5890(8)
c/Å	9.809(2)	11.782(4)	17.244(2)	26.621(2)
α/deg	94.86(1)	109.08(2)	90	102.882(1)
β/deg	111.29(1)	112.68(2)	105.07(2)	95.136(1)
γ/deg	89.59(1)	102.12(2)	90	102.698(1)
V/Å^3	1802.5(5)	1982(1)	4466(2)	4815.9(4)
Z	2	2	4	2
D_{calc}/g cm^{-3}	2.308	2.224	2.266	2.421
μ(Mo $K\alpha$)/cm^{-1}	117.80	105.88	96.79	120.44
Diffractometer	Rigaku AFC7S	Rigaku AFC5R	Rigaku AFC5R	Bruker SMART 1000
λ (Mo $K\alpha$)/Å	0.71073	0.71073	0.71073	0.71073
T/K	233	r.t.	r.t.	213
Crystal size/mm^3	0.20 × 0.20 × 0.10	0.10 × 0.10 × 0.15	0.10 × 0.10 × 0.05	0.15 × 0.10 × 0.05
Unique refrection	8267	9080	4244	21120
Observed	4606	6332	1752	10274
Variables	434	496	267	1079
R	0.053	0.052	0.047	0.057
R_w	0.060	0.064	0.036	0.063
GOF	1.41	2.35	1.34	1.85

Table 2. Selected Bond Distances and Angles for Triplatinum(II) Clusters

Complex	2	3	6	8	
				Site A	Site B
		Bond distances (Å)			
Pt(1)–Pt(2)	2.522(1)	2.5423(9)	2.564(2)	2.548(2)	2.549(1)
Pt(2)–Pt(3)	2.516(1)	2.5291(7)		2.531(1)	2.529(1)
Pt(1)–Pt(3 or 1′)	2.605(1)	2.605(1)	2.592(2)	2.658(1)	2.678(1)
Pt(1)–N(1)	2.13(1)	2.17(1)	2.20(2)	2.20(2)	2.18(2)
Pt(1)–N(2)	2.16(1)	2.14(1)	2.19(2)	2.19(2)	2.23(2)
Pt(2)–N(3)	2.11(2)	2.13(1)	2.22(2)	2.18(2)	2.15(2)
Pt(2)–N(4)	2.09(2)	2.10(1)		2.15(3)	2.18(2)
Pt(3)–N(5)	2.15(1)	2.20(1)		2.16(2)	2.21(2)
Pt(3)–N(6)	2.16(2)	2.17(1)		2.17(2)	2.17(2)
$Pt–N_{av.}$	2.13	2.15	2.20	2.18	2.19
Pt(1)–O(8 or 2)	2.00(1)	1.997(9)	1.99(1)	2.00(1)	2.02(2)
Pt(1)–O(9 or 3)	2.02(1)	2.03(1)	2.01(1)	1.99(2)	2.01(2)
Pt(2)–O(10 or 4)	2.01(1)	2.02(1)	1.98(1)	1.96(2)	2.00(1)
Pt(2)–O(11)	1.99(2)	2.009(9)		1.96(2)	1.97(1)
Pt(3)–O(12)	2.01(1)	2.042(9)		1.96(1)	2.01(2)
Pt(3)–O(13)	2.02(2)	2.00(1)		2.03(1)	2.03(1)
$Pt–O_{av.}$	2.01	2.02	1.99	1.98	2.01
		Bond angles (°)			
Pt(2)–Pt(1)–Pt(3 or 1′)	58.75(3)	58.85(3)	59.65(3)	58.14(4)	57.80(3)
Pt(1)–Pt(2)–Pt(3 or 1′)	62.26(3)	61.81(2)	60.71(5)	63.11(4)	63.65(3)
Pt(1)–Pt(3)–Pt(2)	58.98(3)	59.35(2)		58.75(4)	58.55(3)
N(1)–Pt(1)–N(2)	72.5(7)	74.7(5)	79.6(6)	71.5(8)	71.8(7)
N(3)–Pt(2)–N(4 or 3′)	75.6(7)	75.8(5)	81.4(10)	73.8(9)	71.9(8)
N(5)–Pt(3)–N(6)	73.8(7)	74.4(5)		73.8(8)	71.9(7)

with respect to the cluster plane, which is similar to **1**.

Three dioxime or three Me_2en ligands that have caused the core transformation occupy coordination sites in the cluster plane with chelate mode. Dioxime ligands in **2** and **3** interact via two O–H–O hydrogen bonds over the short edges of the core as shown in dashed lines in Fig. 1a for **2** (O(2)···O(3) = 2.49(2) and O(4)···O(5) = 2.43(2) Å in **2**; O(2)···O(3) = 2.47(2) and O(4)···O(5) = 2.51(2) Å in **3**). On the other hand, no hydrogen bonds operate among the Me_2en ligands in **6**. In both dioxime and Me_2en clusters, however, the out-of-plane unidentate acetate and the in-plane ligands are bound by intramolecular hydrogen bonds, although features of such hydrogen bonds differ. The hydrogen bonds in dioxime clusters, which are again shown in dashed lines in Fig. 1a for **2**, operate over the long edge of the Pt triangle and thereby act as a hydrogen bond bridge (O(1)···O(14) = 2.65(2) and O(6)···O(7) = 2.56(2) Å in **2**, O(1)···O(14) = 2.66(2) and O(6)···O(7) = 2.65(2) Å in **3**). On the other hand, in Me_2en cluster **6**, the hydrogen bonds between the out-of-plane unidentate acetate and the in-plane Me_2en ligands operate between ligands attached to the same Pt atom (O(4)···N(2) = 2.77(2) Å) as shown in dashed lines in Fig. 1b.

The Pt–O distances in these clusters (1.96—2.04 Å) are within a normal range. All the Pt–O bonds are cis to the Pt–Pt bonds and are not affected by the cluster formation. On the other hand, the Pt–N distances in the cluster plane of all the present clusters are clearly longer than those normally found in mononuclear Pt(II) complexes. They range over 2.09—2.20 Å in the dioxime clusters, and those in the Me_2en cluster are 2.19—2.22 Å. The elongation of the Pt–N bonds[19,20] originates from the trans influence of the Pt–Pt bond as in the in-plane coordination bonds of Pt^{II}_4 clusters.[5,7–11] The difference in Pt–N distances between the dioxime and Me_2en clusters is similar to that between the mononuclear Pt(II) complexes with dioxime and diamine ligands.[19,20]

Mechanism of the Cluster Core Transformation from a Square-Planar to a Triangular Type. Figure 2 shows a proposed mechanism of the cluster core transformation. It is based on (i) the common structural features of the Pt_3 clusters, (ii) the regioselective substitution reactivity of $[Pt^{II}_4(\mu\text{-}CH_3COO)_8]$ (**1**), (iii) the stereochemical demand of the incoming ligand that causes the core transformation, and (iv) the structures of the reaction intermediates (see below). In view of the experimental facts thus far discussed, it is reasonable to consider that the first step of the core transformation is the substitution of the in-plane acetates of **1** by the dioxime or Me_2en ligands. In the substitution, the entering dioxime or Me_2en ligands take the chelate coordination mode rather than the bridging mode owing to the stereochemical demand of the incoming ligand. In fact, a molecular model shows that these ligands cannot take the bridge coordination mode in the tetranuclear cluster. As shown in Fig. 2, the coordination of three entering ligands to the Pt_4 cluster core in the chelate mode promotes release of one Pt atom from the square-planar cluster core, which is finally removed completely by free

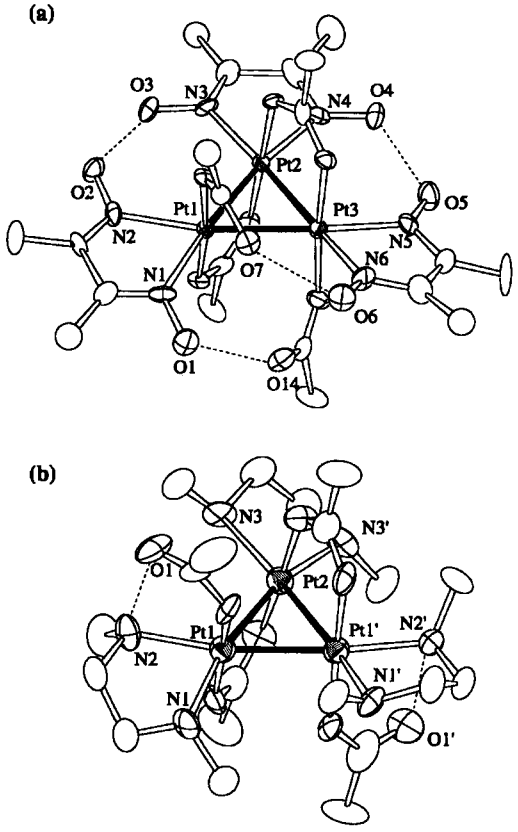

Fig. 1. ORTEP drawing of (a) $[Pt_3(CH_3COO)_4(dmgH)_2(dmgH_2)]$ (**2**) and (b) $[Pt_3(CH_3COO)_4(Me_2en)_3]^{2+}$ (**7**). Thermal ellipsoids are drawn at the 40% probability.

ligands excessively present in the reaction mixture. Four out-of-plane acetates in the starting compound **1**, which are substitution inert, remain at the axial sites of the resulting Pt_3 cluster, acting as bridging ligands or being involved in the hydrogen bond bridge between Pt–Pt bonds (vide ante).

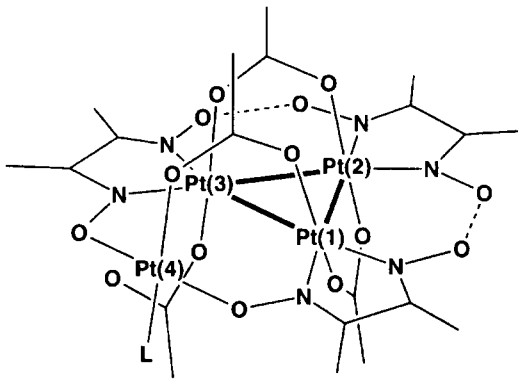

Scheme 1.

We found that a compound regarded as a reaction intermediate is isolated in the reaction of **1** with $dmgH_2$ under milder conditions (room temperature, for 1 d). In fact, this powdery product converted finally to $[Pt_3(CH_3COO)_4(dmgH)_2(dmgH_2)]$ (**2**) in an acetone solution in the presence of an excess of free $dmgH_2$ ligand in a moderate yield. The product was subjected to silica-gel column chromatography and a small amount of the final product **2** was separated out. The resulting compounds, however, showed complicated ^1H NMR spectra, indicating that they are a mixture of some cluster compounds. Fortunately, we obtained single crystals of $[\{Pt_4(CH_3COO)_4(dmgH)_2(dmgH_2)\}_2(\mu\text{-}dmgH_2)]$ (**8**) by diffusing hexane into the CH_2Cl_2 solution of the mixture, and its crystal structure was determined by X-ray analysis. The compound was a dimer of a tetranuclear Pt(II) complex bridged by $dmgH_2$, which has a quasi-C_2 axis at the center of dimer (Fig. 3). Selected bond distances and angles are given in Table 2.[21] The structure of a half of the molecule is illustrated schematically in Scheme 1. The tetranuclear Pt(II) core consists of two units, a triangular cluster unit very similar to **2**

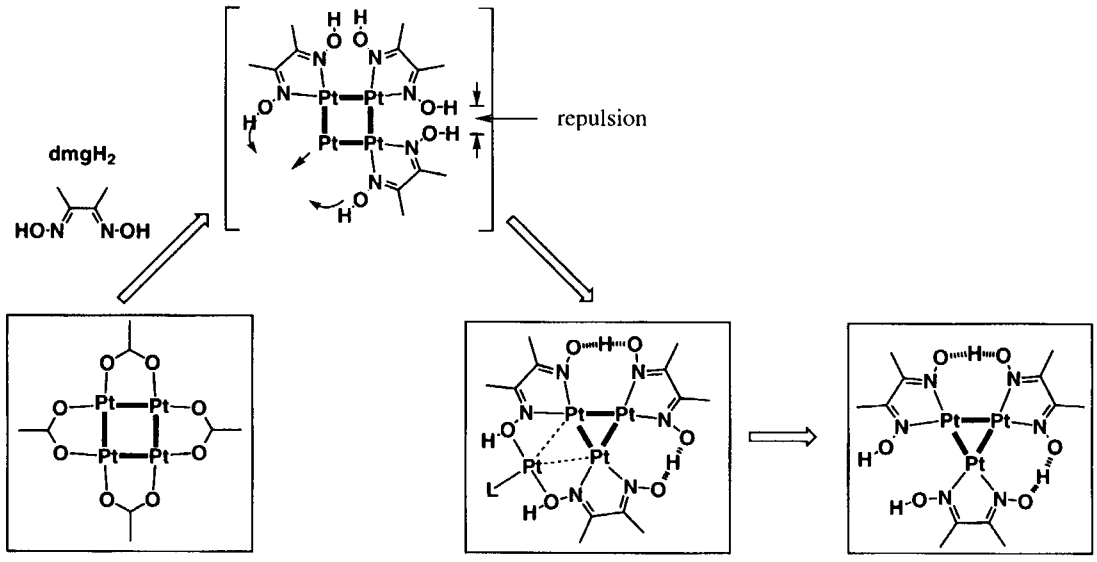

Fig. 2. Mechanism of cluster core transformation from the tetranuclear to trinuclear type. Out-of-plane ligands are omitted for clarify.

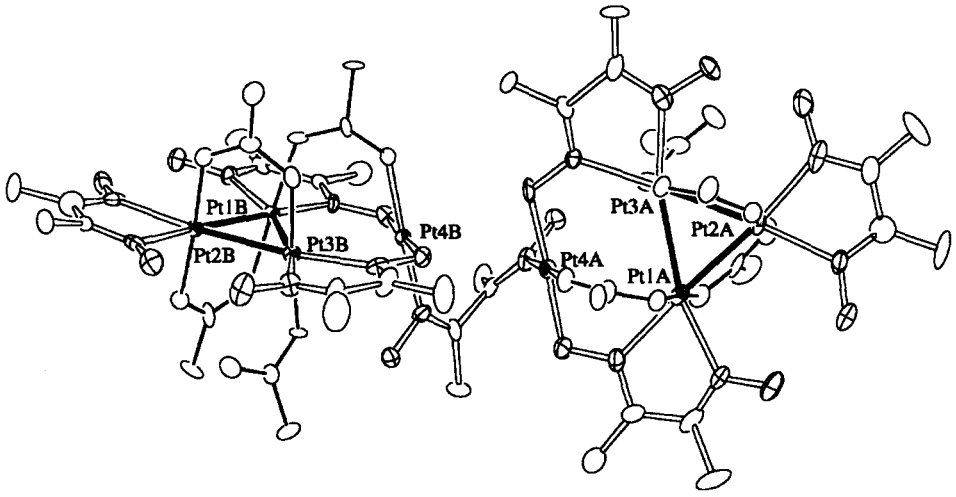

Fig. 3. ORTEP drawing of [{$Pt_4(CH_3COO)_4(dmgH)_2(dmgH_2)\}_2(\mu$-$dmgH_2)$] (**8**). Thermal ellipsoids are drawn at the 20% probability.

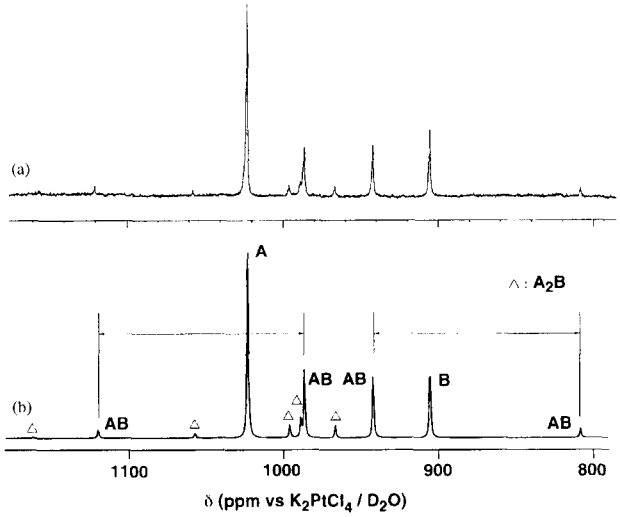

Fig. 4. Observed (a) and calculated (b) ^{195}Pt NMR spectra of [$Pt_3(CH_3COO)_4(bqdH)_2(bqdH_2)$] (**5**) in $CDCl_3$.

and a mononuclear unit with square planar geometry. There are no Pt–Pt bonds between the units. The cluster core comprised of Pt(1), Pt(2), and Pt(3) is an isosceles triangle with dimensions very similar to those of **2** (Table 2). When Pt(4) in the mononuclear unit and the ligand L are removed from the structure in Scheme 1, a residual structure is essentially the same as **2**. The disposition of the four out-of-plane acetates in **1** remains almost unchanged in the intermediate. The structure of the intermediate shows the partial removal of one Pt atom from the tetranuclear cluster core of **1**. In the reaction intermediate **8**, $dmgH_2$ assumes the L site to give the dimer of the molecule, as shown in Scheme 1. The structural feature of the reaction intermediate is consistent with the proposed mechanism in Fig. 2. In the tetranuclear reaction intermediate, various unidentate ligands can occupy the site designated as L in Scheme 1. In fact, a compound other than **8** that has the structure shown in Scheme 1 is isolated from this mixture of intermediate.[22] Such an intermediate was not obtained in reaction of **1** with other dioximes.

^{195}Pt NMR of Trinuclear Platinum(II) Clusters. ^{195}Pt NMR is a powerful tool for the study of platinum cluster complexes with Pt–Pt bond(s).[23,24] ^{195}Pt NMR spectra for such compounds, however, are in general complicated because of the presence of isotopomers (natural abundance of ^{195}Pt = 33.8%) and large Pt–Pt coupling constants. Furthermore, when a coupling constant is large relative to the chemical shift difference, a second order pattern is observed. Because of the presence of isotopomers, ^{195}Pt NMR spectrum for a species with Pt–Pt bond(s) results from the sum of resonance(s) of each isotopomer.

The present Pt_3 clusters show such a ^{195}Pt NMR spectral pattern. As an example, a spectrum of [$Pt_3(CH_3COO)_4(bqdH)_2(bqdH_2)$] (**5**) in $CDCl_3$ is shown in Fig. 4a. The observed spectrum was analyzed in the following way. This cluster has two kinds of ^{195}Pt nuclei with different chemical shifts, as evidenced by C_2 symmetry of ^{1}H- and ^{13}C NMR or the isosceles triangle structure of the cluster core. Therefore the spectrum should be of three spin system of A_2B type. Figure 5 shows eight possible isotopomers, their classification into six types, and their natural abundance for this cluster. Isotopomer (a) has no ^{195}Pt nucleus and shows no ^{195}Pt NMR resonance. Both (b) and (c) isotopomers show a singlet peak at the same position

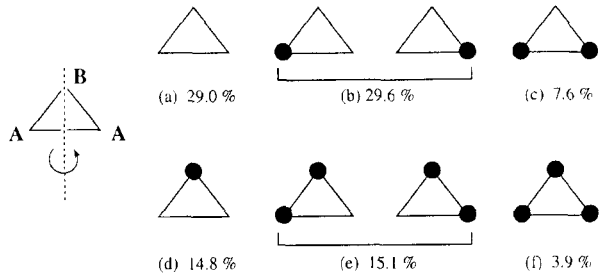

Fig. 5. Eight possible isotopomers and their classification into six types (a)—(f) for a Pt_3 cluster with C_2 symmetry. An isosceles triangle denotes a trinuclear cluster core, and a filled circle shows the position of ^{195}Pt nucleus. The percentages are natural abundance of the isotopomers.

(singlet A). Isotopomer (d) also shows a singlet (singlet B) at a different position from the singlet A. Isotopomer (e) has directly bonded ^{195}Pt nuclei and coupling constant $^{1}J_{Pt-Pt}$ would be large relative to a chemical shift difference. Therefore the type (e) isotopomers should show an AB quartet. Isotopomer (f) has three mutually coupled ^{195}Pt nuclei and should show many signals of A_2B pattern with weak intensity because of the spread of the total intensity and of the low abundance. The observed ^{195}Pt NMR spectrum of $[Pt_3(CH_3COO)_4(bqdH)_2(bqdH_2)]$ (**5**) is the sum of spectra of the A, B, AB, and A_2B type, where these components have their own spectral intensities governed by the natural abundance of isotopomers given in Fig. 5. If the natural abundance of ^{195}Pt is assumed to be an approximate value of 1/3, the spectrum should consist of two main singlets A and B with a relative intensity ratio of 12 : 4, an AB pattern with relative intensity ratio of 8 in total, in addition to weak A_2B type signals with intensity ratio of 3 in total.[25] In actual fact, such a spectral pattern can be seen in Fig. 4a. Two singlets A and B and an AB pattern are easily identified from the relative intensities and their signal pattern and positions (δ_A = 1023.4 ppm and δ_B = 905.7 ppm). A coupling constant $^{1}J_{AB}$ obtained from peak separation between inner and outer peak positions of the AB pattern was 7750 Hz. In addition to these signals, some main signals of A_2B spectrum can also be identified around 1000 ppm. A spectrum simulation was carried out with use of the observed chemical shifts and coupling constant (Fig. 4b). The good agreement between the observed and simulated spectra indicates the validity of the analysis.

The ^{195}Pt NMR spectra of other Pt_3 clusters were successfully analyzed in the same way, and the assignments and coupling constants are given in Table 3. Chemical shifts of Pt_3 clusters with dioxime ligand **2**—**5** are around at 1000 ppm (vs. K_2PtCl_4/D_2O) and are similar to those of the Pt_4 clusters with oxygen or nitrogen donors.[9,11,24] Chemical shift differences between Pt_A and Pt_B nuclei in the dioxime clusters are 3.6, 27.8, 20.8, and 117.7 ppm for **2**—**5**, respectively. The order appears to be related to the stereochemical rigidity of the dioxime ligand, which might affect a distortion of the cluster core structure. On the other hand, the chemical shift difference in **6** was 272.9 ppm, which is much larger than those in the dioxime clusters. The reason may be ascribed to a difference in intramolecular hydrogen bonds within the clusters (vide ante). As given in Table 3, coupling constants J_{AB} of the present Pt_3 clusters are very large (ca. 8000 Hz). The magnitudes are similar to those of the Pt_4 clusters,[11,24] and suggest the presence of Pt–Pt bonds.

EHMO Calculations. EHMO calculations have been carried out for a triangular model compound, $[Pt^{II}_3(HCOO)_4(glyH)_2(glyH_2)]$ ($glyH_2$ = glyoxime) and its 1/3 fragment. The method of calculations is the same as reported for $[Pt^{II}_4(HCOO)_8]$.[7] Geometry of the molecules including the Pt_3 isosceles triangle is based on the X-ray structures. Figure 6 shows calculated energy levels associated with Pt 5d orbitals for $[Pt^{II}_3(HCOO)_4(glyH)_2(glyH_2)]$ and the 1/3 fragment, and their correlation. A relatively large HOMO-LUMO gap (1.67 eV) suggests the stability of the triangular cluster core. We will discuss here only molecular orbitals derived from d_σ orbitals ("$d_{x^2-y^2}$" and "d_{z^2}")[26] of

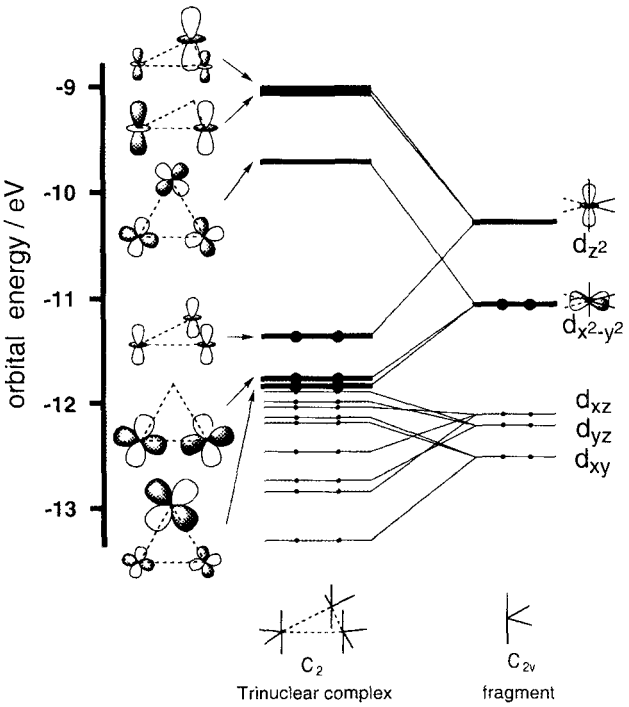

Fig. 6. Extended Hückel molecular orbital diagram for a model trinuclear cluster, $[Pt^{II}_3(HCOO)_4(glyH)_2(glyH_2)]$, and its 1/3 fragment.

Table 3. ^{195}Pt NMR Chemical Shifts (δ vs. K_2PtCl_4/D_2O) and Coupling Constants (J_{Pt-Pt}) for Triplatinum(II) Clusters

Compound	Solvent	δ_A[a)]	δ_B[b)]	J_{Pt-Pt}/Hz
$[Pt_3(CH_3COO)_4(dmgH_2)(dmgH)_2]$ (**2**)	$CDCl_3$	1035.1	1038.7	c)
$[Pt_3(CH_3COO)_4(cdoH_2)(cdoH)_2]$ (**3**)	$CDCl_3$	1047.8	1020.0	7670
$[Pt_3(CH_3COO)_4(dpgH_2)(dpgH)_2]$ (**4**)	$CDCl_3$	974.6	995.4	7890
$[Pt_3(CH_3COO)_4(bqdH_2)(bqdH)_2]$ (**5**)	$CDCl_3$	1023.4	905.7	7750
$[Pt_3(CH_3COO)_4(Me_2en)_3]^{2+}$ (**6**)	D_2O	1189.2	916.4	8060
$[Pt_3(CH_3COO)_4(en)_3]^{2+}$ (**7**)[d)]	D_2O	1058.8	834.1	7570

a) Pt at the unique apex of the Pt_3 isoscelese triangle. b) Pt atoms at both the ends of long edge of the Pt_3 isoscelese triangle. c) not determined. d) This compound was prepared from a reaction of **3** with an excess of en in D_2O solution (see text).

the fragment, which are shown in thick lines in the diagram. Molecular orbitals derived from d_π ("d_{xy}", "d_{xz}", "d_{yz}") orbitals of the fragment are fully occupied and bonding and antibonding effects are compensated in the whole molecule. The "d_{z^2}" orbital of the fragment make three molecular orbitals, one bonding and two antibonding orbitals, the latter of which are nearly degenerate. Three "$d_{x^2-y^2}$" of the fragments form one antibonding and two closely separated bonding orbitals. Each fragment has two d_σ electrons and then the cluster has six d_σ electrons, which occupy the low lying three bonding orbitals. This means the presence of three Pt–Pt single bonds between neighboring Pt atoms in the triangular framework. Moreover, reduced overlap populations between adjacent platinum atoms in the Pt_3 isosceles triangular core were 0.355 and 0.332. The magnitudes suggest also the existence of metal–metal bonds between platinum atoms.

Solution Behavior of Pt_3 Clusters. (i) Species in Solution. Dioxime clusters **2**—**5** show ^{1}H-, ^{13}C-, and ^{195}Pt NMR spectra with C_2 symmetry, indicating that the solid state structure is retained in solution state. On the other hand, diamine cluster **6** shows complicated ^{1}H- and ^{195}Pt NMR spectra in D_2O. When an excess of free diamine ligand was added to the NMR sample solution, however, a spectrum with C_2 symmetry typical of the Pt_3 cluster was obtained. This indicates that diamine ligand in **6** dissociates partly to give an equilibrium mixture in aqueous solution.

(ii) Reactivity of In-Plane Ligand Substitution. It is now well established that tetranuclear Pt(II) cluster $[Pt_4(CH_3COO)_8]$ (**1**) shows remarkable regioselective ligand substitution: the acetate ligands which are in the plane of the square-planar cluster core are labile, whereas the out-of-plane ligands are inert to substitution.[5,8–11] The regioselective substitution originates from the strong trans effect of Pt–Pt bonds in the Pt_4 cluster core. Similar regioselective substitution is expected for the present Pt_3 clusters which have Pt–Pt bonds. We investigated substitution reactions for the series of Pt_3 complexes with use of various incoming bidentate ligands such as carboxylate, diamine, and oxime. We found that some Pt_3 clusters undergo in-plane ligand substitution, and that the out-of-plane acetate ligands are inert to substitution as in **1**.

Reaction of $[Pt_3(CH_3COO)_4(cdoH)_2(cdoH_2)]$ (**3**) with an excess of Me_2en affords $[Pt_3(CH_3COO)_4(Me_2en)_3]^{2+}$ (**6**) (Eq. 3).[27]

$$[Pt_3(CH_3COO)_4(cdoH)_2(cdoH_2)] + 3\ Me_2en + 2\ H_2O \longrightarrow [Pt_3(CH_3COO)_4(Me_2en)_3]^{2+} + 3\ cdoH_2 + 2\ OH^- \quad (3)$$

A D_2O solution of $[Pt_3(CH_3COO)_4(Me_2en)_3]^{2+}$ (**6**) in the presence of an excess of ethylenediamine shows ^{195}Pt NMR spectrum corresponding to $[Pt_3(CH_3COO)_4(en)_3]^{2+}$ (**7**). On the other hand, the substitution of dioxime clusters with some other dioxime ligand proceeds but does not afford fully substitution of the oxime ligands. A reaction of $[Pt_3(CH_3COO)_4(cdoH)_2(cdoH_2)]$ (**3**) with an excess of $dpgH_2$ under refluxing for 24 h gave a mixture of unreacted cluster **3** and partially substituted derivatives, $[Pt_3(CH_3COO)_4(dpgH)_n(cdoH)_{2-n}(cdoH_2)]$ (n = 1 and/or 2), but did not afford a fully substituted cluster $[Pt_3(CH_3COO)_4(dpgH)_2(dpgH_2)]$ (**4**). Prolonged refluxing of the reaction mixture did not afford **4**, but resulted in decomposition of cluster **3**. Reaction of a contrary pair, that is, reaction of **4** with free $cdoH_2$ ligand, gave very similar results. These facts indicate that the in-plane ligand substitution does occur in solution. Substitution reactivity of the Pt_3 clusters was, however, much lower than that of **1** in general, and severer conditions such as higher temperature or prolonged reaction time were required. The reason would be attributed in principle to strong intramolecular hydrogen bonds in the Pt_3 clusters. The driving force for the regioselective substitution is again the trans effect of the Pt–Pt bonds in the clusters, and therefore acetate ligands are inert to substitution.

Experimental

Materials. $[Pt_4(CH_3COO)_8]$ (**1**) was prepared by the literature method.[28] Organic solvents were dried on molecular sieve 4A before use. Deuterated solvents and other reagents were used as received.

Apparatus. ^{1}H, ^{13}C, ^{195}Pt NMR spectra were recorded on a JEOL GSX-270 FT-NMR spectrometer at 270, 67.9, and 58.0 MHz, respectively. Elemental analyses and measurements of FAB-mass spectra (JEOL JMS-HX100) were carried out at Instrumental Analysis Center, Tohoku University.

Synthesis of $[Pt_3(CH_3COO)_4(dmgH)_2(dmgH_2)]$ (2). Method A. To an acetone solution (30 cm^3) of **1** (100 mg) was added an acetone solution (30 cm^3) of $dmgH_2$ (500 mg) and the solution was refluxed for 4 h. The blue black precipitate which formed was filtered off and the filtrate was evaporated to dryness. The residue was dissolved in dichloromethane (2 cm^3) and the filtered solution was charged onto silica-gel column (Wakogel C-200). On elution of dichloromethane/methanol (97 : 3), the first brown fraction was collected. The effluent was evaporated and purified by gel-filtration column (Sephadex LH-20, dichloromethane/acetonitrile (2/1) as eluent) to give brown powder (yield 27 mg, 30%).

Method B. To an acetone solution (20 cm^3) containing 50 mg of mixture **A** (see section for isolation of **8**) was added an acetone solution (20 cm^3) of $dmgH_2$ (50 mg) and the solution was refluxed for 4 h. The blue black precipitate which formed was filtered off and the filtrate was evaporated to dryness. The residue was dissolved in dichloromethane (2 cm^3) and the filtered solution was charged onto a silica-gel column (Wakogel C-200). On elution of dichloromethane/methanol (97 : 3) the first brown fraction was collected. The effluent was evaporated to give brown powder (yield 15 mg, 37%).

Data for **2**: ^{1}H NMR (270 MHz, $CDCl_3$) δ = 1.79 (s, 6H, OAc–CH_3), 1.85 (s, 6H, OAc–CH_3), 2.35 (s, 6H, dmg–CH_3), 2.40 (s, 6H, dmg–CH_3), 2.44 (s, 6H, dmg–CH_3), 12.22 (s, 2H, dmg-OH); ^{13}C NMR (67.9 MHz, $CDCl_3$, TMS) δ = 12.77 (dmg–CH_3), 12.94 (dmg–CH_3), 13.16 (dmg–CH_3), 21.25 (OAc–CH_3), 21.62 (OAc–CH_3), 149.31 (dmg–C=N), 150.33 (dmg–C=N), 155.59 (dmg–C=N), 179.58 (OAc–CO), 192.07 (OAc–CO); MS(FAB) *m/z* 1167 (Calcd for M^+: 1167.6). Anal. Found: C, 21.47; H, 3.13; N, 6.93%. Calcd for **2**·2CH_3OH = $Pt_3C_{22}H_{42}N_6O_{16}$: C, 21.45; H, 3.44; N, 6.82%.

Dark brown crystals of **2**·CH_2Cl_2 suitable for X-ray analysis were grown by slow diffusion of hexane into a dichloromethane

solution of **2**.

Synthesis of $[Pt_3(CH_3COO)_4(cdoH)_2(cdoH_2)]$ (3). To an acetonitrile solution (30 cm^3) of **1** (200 mg) was added an acetonitrile solution (130 cm^3) of cyclohexanedione dioxime $cdoH_2$ (430 mg) and the mixture was stirred for 12 h. The brown needle crystals which formed were removed by filtration and the filtrate was evaporated to dryness. The residue was dissolved in dichloromethane (5 cm^3) and the filtered solution was charged onto a silica-gel column (Wakogel C-200). On elution of dichloromethane/methanol (98 : 2) the main brown fraction was collected. The effluent was evaporated and purified by gel-filtration column (Sephadex LH-20, dichloromethane/acetonitrile (2/1) as eluent) to give brown powder (yield 150 mg, 70%). ^{1}H NMR (270 MHz, $CDCl_3$) δ = 1.81 (s, 6H, OAc–CH_3), 1.86 (s, 6H, OAc–CH_3), 1.73 (m, 12H, cdo–CH_2), 2.97 (m, 12H, cdo–CH_2), 12.08 (s, 2H, cdo–OH); ^{13}C NMR (67.9 MHz, $CDCl_3$) δ = 21.29 (cdo–CH_2), 21.34 (cdo–CH_2), 21.42 (cdo–CH_2), 21.68 (OAc–CH_3), 25.69 (cdo–CH_2), 25.77 (cdo–CH_2), 25.84 (cdo–CH_2), 149.94 (cdo–C=N), 151.22 (cdo–C=N), 156.03 (cdo–C=N), 179.55 (OAc–CO), 192.06 (OAc–CO); MS(FAB) *m/z* 1246 (Calcd for M^+: 1245.7). Anal. Found: C, 25.33; H, 3.28; N, 6.59%. Calcd for $Pt_3C_{26}H_{40}N_6O_{14}$: C, 25.07; H, 3.24; N, 6.75%.

Red crystals of **3**·2CH_3CN suitable for X-ray analysis were obtained by recrystallization from acetonitrile solution of **3**.

Synthesis of $[Pt_3(CH_3COO)_4(dpgH)_2(dpgH_2)]$ (4). To an acetonitrile solution (15 cm^3) of **1** (100 mg) was added an acetonitrile solution (80 cm^3) of $dpgH_2$ (1 g) and the mixture was stirred for 12 h. The blue and white solids which formed were removed by filtration and the filtrate was evaporated to dryness. The residue was dissolved in dichloromethane (3 cm^3) and the filtered solution was charged onto a silica-gel column (Wakogel C-200). On elution of dichloromethane/methanol (99 : 1), the main dark brown fraction (Fr. 4) was collected and evaporated to give brown powder (yield 55 mg, 45%). ^{1}H NMR (270 MHz, $CDCl_3$) δ = 1.92 (s, 6H, OAc–CH_3), 1.97 (s, 6H, OAc–CH_3), 7.24—8.04 (m, 30H, dpg–ϕ), 12.79 (s, 2H, dpg–OH); ^{13}C NMR (67.9 MHz, $CDCl_3$) δ = 21.34 (OAc–CH_3), 21.90 (OAc–CH_3), 126.28—130.63 (dpg–ϕ), 151.17 (dpg–C=N), 151.58 (dpg–C=N), 155.52 (dpg–C=N), 179.64 (OAc–CO), 192.51 (OAc–CO); MS(FAB) *m/z* 1540 (Calcd for M^+: 1539.2). Anal. Found: C, 39.44; H, 3.15; N, 5.42%. Calcd for $Pt_3C_{50}H_{46}N_6O_{14}$: C, 38.99; H, 2.99; N, 5.46%.

Synthesis of $[Pt_3(CH_3COO)_4(bqdH)_2(bqdH_2)]$ (5). To an acetonitrile solution (15 cm^3) of **1** (100 mg) was added an acetonitrile solution (30 cm^3) of $bqdH_2$ (55 mg) and the mixture was stirred for 10 min. The black solids which formed were removed by filtration and the filtrate was evaporated to dryness. The residue was dissolved in dichloromethane (5 cm^3) and the solution filtered was charged onto a silica-gel column (Wakogel C-200). On elution of dichloromethane/methanol (97 : 3), the main dark brown fraction (Fr. 4) was collected and evaporated to give brown powder (yield 25 mg, 25%). ^{1}H NMR (270 MHz, $CDCl_3$) δ = 1.79 (s, 6H, OAc–CH_3), 1.85 (s, 6H, OAc–CH_3), 6.53—6.74 (m, 6H, bqd–ϕ), 7.26—7.41 (m, 6H, bqd–ϕ), 12.49 (s, 2H, bqd–OH); ^{13}C NMR (67.9 MHz, $CDCl_3$) δ = 21.20 (OAc–CH_3), 21.66 (OAc–CH_3), 118.11 (bqd–ϕ), 118.54 (bqd–ϕ), 118.79 (bqd–ϕ), 127.95 (bqd–ϕ), 130.46 (bqd–ϕ), 133.30 (bqd–ϕ), 147.97 (bqd–C=N), 149.61 (bqd–C=N), 151.29 (bqd–C=N), 179.76 (OAc–CO), 192.30 (OAc–CO); MS(FAB) *m/z* 1234 (Calcd for M^+: 1233.1). Anal. Found: C, 25.05; H, 2.14; N, 6.80%. Calcd for $Pt_3C_{26}H_{28}N_6O_{14}$: C, 25.31; H, 2.29; N, 6.81%.

Synthesis of $[Pt_3(CH_3COO)_4(Me_2en)_3]^{2+}$ (6). Method A. To a dichloromethane solution (5 cm^3) of **1** (100 mg) was added 0.1 cm^3 of Me_2en. The color of the solution changed from red to dark brown and white powder was precipitated. After 24 h, the precipitates were filtered off and the filtrate was evaporated to give a brown oil. To this oil was added 3 cm^3 of water and 200 mg of sodium perchlorate. The solution was slowly evaporated for several days to give dark red crystals of the perchlorate salt.

Data for **6**$(ClO_4)_2$: Anal. Found: C, 18.90; H, 3.65; N, 6.51; Cl, 5.85%. Calcd for $Pt_3C_{20}H_{48}N_6O_{16}Cl_2$: C, 18.70; H, 3.77; N, 6.54; Cl, 5.52%.

Method B. To a dichloromethane solution (5 cm^3) of **3** (100 mg) was added 0.17 cm^3 of Me_2en. The color of the solution changed from red to dark brown and white powder was precipitated. After 24 h, the precipitate was filtered off and the filtrate was evaporated to give a brown oil. ^{195}Pt NMR of D_2O solution of this oily material shows the same spectrum as that of **6**.

Dark red crystals of **6**$(ClO_4)_2$·2$NaClO_4$ suitable for X-ray work were obtained by recrystallization from aqueous solution of **6**$(ClO_4)_2$ containing an excess of $NaClO_4$.

Caution! The perchlorate salts are potentially explosive. Small quantities only should be prepared and precautions taken during handling.

Formation of $[Pt_3(CH_3COO)_4(en)_3]^{2+}$ (7) in Solution. To a dichloromethane solution (5 cm^3) of **3** (100 mg) was added 0.17 cm^3 of ethylenediamine. The color of the solution changed from red to dark brown and white powder was precipitated. After 24 h, the precipitates were filtered off and the filtrate was evaporated to give a brown oil. ^{195}Pt NMR of this oily material in D_2O solution was typical of the Pt_3 cluster.

Isolation of $[\{Pt_4(CH_3COO)_4(dmgH)_2(dmgH_2)\}_2(\mu$-$dmgH_2)]$·8$CH_2Cl_2$ (8·8CH_2Cl_2). To an acetone solution (180 cm^3) of **1** (500 mg) was added an acetone solution (150 cm^3) of $dmgH_2$ (2.5 g) and the mixture was stirred for 20 h. Brown needle crystals which formed were removed by filtration and the filtrate was evaporated to dryness. The residue was dissolved in dichloromethane (20 cm^3) and the filtered solution was charged onto a silica-gel column (Wakogel C-200). On elution of dichloromethane/methanol (97 : 3) the third main brown fraction was collected. The effluent was evaporated to give brown powder, which was found by NMR to be a mixture of some platinum clusters (mixture **A**, yield 250 mg). Dark brown crystals of $[\{Pt_4(CH_3COO)_4(dmgH)_2(dmgH_2)\}_2(\mu$-$dmgH_2)]$·8$CH_2Cl_2$ (**8**·8CH_2Cl_2) suitable for X-ray work were picked up from the products obtained by slow diffusion of hexane into the CH_2Cl_2 solution of mixture **A**.

X-Ray Crystallography. Data collections and structure analyses were made commonly in the following way. A suitable crystal coated with epoxy glue was attached to a glass fiber and mounted on a Rigaku AFC 7S or Rigaku AFC 5S four circle diffractometer or a Bruker SMART 1000 CCD detector. Lorentz, polarization, and absorption corrections (Ψ-scan, DIFABS,[29] or numerical integration) were applied to the intensity data. The structure was solved by the automatic Patterson analysis (DIRDIF PATTY[30]) and successive difference Fourier, and refined by the full matrix least-squares method. Anisotropic temperature factors were applied to all non-hydrogen atoms. All calculations were performed with use of the teXsan crystallographic software package.[31] Crystallographic data (excluding structure factors) for the structures in this paper have been deposited with the Cambridge Crystallographic Data Centre as supplementary publication Nos. CCDC 135678-135681. Copies of the data can be obtained, free of charge, on application to CCDC, 12 Union Road, Cambridge CB2 1EZ, UK. The data are also deposited as Document No. 73028 at the Office of the Editor of Bull. Chem. Soc. Jpn.

Simulation of ^{195}Pt NMR Spectra. Calculations of peak po-

sitions and relative intensities in second order ^{195}Pt NMR spectrum for each isotopomer were performed with the program LAOCN5.[32] The chemical shifts used in the calculation were obtained directly from the positions of two main singlets in the observed spectrum. The coupling constants J_{Pt-Pt} were obtained directly from difference between outer and inner peak positions of AB pattern when outer peak(s) of AB pattern was clearly observed. When the outer peak of AB pattern was too weak to read out the position, the coupling constant was calculated from a chemical shift separation between singlets A and B and a separation between inner peaks of AB pattern. In the simulated spectrum, each signal was drawn at a calculated position with calculated relative intensity based on the natural abundance of isotopomer(s).

This work was supported by Grant-in-Aid for Scientific Research (No. 10740299 and Priority Areas No. 10149102 "Metal-Assembled Complexes") from the Ministry of Education, Science, Sports and Culture.

References

1 a) J. C. Calabrese, L. F. Dahl, P. Chini, G. Longoni, and S. Martinengo, *J. Am. Chem. Soc.*, **96**, 2614 (1974). b) B. K. Teo, F. J. Disalvo, J. V. Waszczak, G. Longoni, and A. Ceriotti, *Inorg. Chem.*, **25**, 2262 (1986).

2 a) R. Bender, P. Braunstein, A. Tiripicchio, and M. T. Camellini, *Angew. Chem., Int. Ed. Engl.*, **24**, 861 (1985). b) G. Ferguson, B. R. Lloyd, and R. J. Puddephatt, *Organometallics*, **5**, 334 (1986). c) Y. Yamamoto, H. Yamazaki, and T. Sakurai, *J. Am. Chem. Soc.*, **104**, 2329 (1982). d) A. Albinati, A. Moor, P. S. Pregosin, and L. M. Venanzi, *J. Am. Chem. Soc.*, **104**, 7672 (1982). e) R. Ramachandran, D. S. Yang, N. C. Payne, and R. J. Puddephatt, *Inorg. Chem.*, **31**, 4236 (1992). f) T. Tanase, H. Ukaji, H. Takahata, H. Toda, T. Igoshi, and Y. Yamamoto, *Organometallics*, **17**, 196 (1998). g) T. Zhang, M. Drouin, and P. D. Harvey, *Inorg. Chem.*, **38**, 957 (1999).

3 a) R. J. Puddephatt, *Chem. Soc. Rev.*, **12**, 99 (1983). b) J. V. Krevor, U. Simonis, A. Karson, C. Castro, and M. Aliakbar, *Inorg. Chem.*, **31**, 312 (1992), and references cited therein.

4 a) J. D. Woollins and P. F. Kelly, *Coord. Chem. Rev.*, **65**, 115 (1985). b) T. V. O'Halloran and S. J. Lippard, *Isr. J. Chem.*, **25**, 130 (1985). c) F. A. Cotton and R. A. Walton, *Struct. Bonding (Berlin)*, **62**, 1 (1985). d) F. A. Cotton, L. R. Falvello, and S. Han, *Inorg. Chem.*, **21**, 1709 (1982). e) T. G. Appleton, K. A. Byriel, J. R. Hall, C. H. L. Kennard, and M. T. Mathieson, *J. Am. Chem. Soc.*, **114**, 7305 (1992); K. Umakoshi and Y. Sasaki, *Adv. Inorg. Chem.*, **40**, 187 (1993); K. Umakoshi and Y. Sasaki, *Inorg. Chem.*, **36**, 4296 (1997).

5 T. Yamaguchi, Y. Sasaki, and T. Ito, *J. Am. Chem. Soc.*, **112**, 4038 (1990).

6 a) T. V. O'Halloran, P. K. Mascharak, I. D. Williams, M. M. Roberts, and S. J. Lippard, *Inorg. Chem.*, **26**, 1261 (1987). b) K. Sakai, Y. Tanaka, Y. Tsuchiya, K. Hirata, T. Tsubomura, S. Iijima, and A. Bhattacharjee, *J. Am. Chem. Soc.*, **120**, 8366 (1998). c) K. Sakai, M. Takeshita, Y. Tanaka, T. Ue, M. Yanagisawa, K. Kosaya, T. Tsubomura, M. Ato, and T. Nakano, *J. Am. Chem. Soc.*, **120**, 11353 (1998), and references cited therein.

7 a) M. A. A. F. de C. T. Carrondo and A. C. Skapski, *J. Chem. Soc., Chem. Commun.*, **1976**, 410. b) M. A. A. F. de C. T. Carrondo and A. C. Skapski, *Acta Crystallogr., Sect. B*, **B34**, 1857 (1978). c) M. A. A. F. de C. T. Carrondo and A. C. Skapski, *Acta Crystallogr., Sect. B*, **B34**, 3576 (1978).

8 T. Yamaguchi, Y. Sasaki, A. Nagasawa, T. Ito, N. Koga, and K. Morokuma, *Inorg. Chem.*, **28**, 4311 (1989).

9 T. Yamaguchi, T. Ueno, and T. Ito, *Inorg. Chem.*, **32**, 4996 (1993).

10 T. Yamaguchi, A. Shibata, and T. Ito, *J. Chem. Soc., Dalton Trans.*, **1996**, 4031.

11 A. Shibata, T. Yamaguchi, and T. Ito, *Inorg. Chim. Acta*, **265**, 197 (1997).

12 T. Yamaguchi, H. Adachi, Y. Sasaki, and T. Ito, *Bull. Chem. Soc. Jpn.*, **67**, 3116 (1994).

13 In this context, we denote formally trinuclear platinum complex with dioxime ligands as $[Pt_3(CH_3COO)_4(dioxH)_2(dioxH_2)]$. This dose not mean an exclusion of a related structure, $[Pt_3(CH_3COO)_4(diox)](dioxH_2)_2$, since the structures contain H bond and the positions of hydrogen atoms are not detrmined.

14 T. Yamaguchi, N. Nishimura, and T. Ito, *J. Am. Chem. Soc.*, **115**, 1612 (1993).

15 It has been confirmed that a mononuclear complex $[Pt(dmgH)_2]$ is precipitated during reaction (1).

16 Diaminoglyoxime ($dagH_2$) also undergoes the same type of reaction to give $[Pt_3(CH_3COO)_4(dagH)_2(dagH_2)]$. Overall structure of this cluster is very similar to those of **2**—**5** and structural data are deposited as Document No. 73028 at the Office of the Editor of Bull. Chem. Soc. Jpn.

17 pK_a: dmg 13.53, cdo 13.11, dpg 10.3, bqd 6.93.

18 In the case of the Pt_4 cluster with C donor atoms, $[Pt_4(CH_3COO)_4(acac)_4]$, Pt–Pt distances are 2.578(1) and 2.595(1) Å owing to strong trans influence of the C donor (Ref. 12).

19 A Pt–N distance in mononuclear dioxime complex is ca. 2.00 Å. For example: E. Frasson, C. Panattoni, and R. Zannetti, *Acta Crystallogr.*, **12**, 1027 (1959).

20 A Pt–N distance in mononuclear diamine complex is ca. 2.05 Å. For example: W. A. Freeman, *Inorg. Chem.*, **15**, 2235 (1976).

21 Other relevant atomic distances (Å): Pt(1A)–Pt(4A) = 3.251(1), Pt(3A)–Pt(4A) = 3.364(1), Pt(1B)–Pt(4B) = 3.235(1), Pt(3B)–Pt(4B) = 3.359(1), Pt(4A)–O(1A) = 1.97(2), Pt(4A)–O(6A) = 1.99(2), Pt(4A)–O(7A) = 2.01(1), Pt(4A)–N(7) = 1.98(2), Pt(4B)–O(1B) = 2.01(1), Pt(4B)–O(6B) = 1.97(1), Pt(4B)–O(7B) = 2.04(1), Pt(4B)–N(8) = 1.98(2).

22 In the earlier communication,[14] we reported that $[Pt_4(CH_3COO)_5(dmgH)_3]$ was isolated from the intermediate, that its structure is the same as that in Scheme 1, and that one of the acetate ligands, which corresponds to L in Scheme 1, could not be determined clearly. We carried out X-ray analysis with use of a different specimen of this compound, but we fail to identify L in $[Pt_4(CH_3COO)_4(dmgH)_2(dmgH_2)(L)]$.

23 a) J. C. Calabrese, L. F. Dahl, P. Chini, G. Longoni, and S. Martinengo, *J. Am. Chem. Soc.*, **96**, 2614 (1974). b) B. K. Teo, F. J. Disalvo, J. V. Waszczak, G. Longoni, and A. Ceriotti, *Inorg. Chem.*, **25**, 2262 (1986).

24 T. Yamaguchi, K. Abe, and T. Ito, *Inorg. Chem.*, **33**, 2689 (1994).

25 Relative spectral intensities are expressed as follows. For singlet A: contribution from isotopomers (b) $\{ = [1\times(1/3)\times(2/3)\times(2/3)]\times 2\}$ + contribution from isotopomer (c) $\{ = [2\times(1/3)\times(1/3)\times(2/3)]\} = 12/27$; For singlet B (isotopomer (d): $[1\times(1/3)\times(2/3)\times(2/3)] = 4/27$; For the AB type: $[2\times(2/3)\times(1/3)\times(1/3)]\times 2 = 8/27$; For the A_2B type: $[3\times(1/3)\times(1/3)\times(1/3)] = 3/27$.

26 The "$d_{x^2-y^2}$" and "d_{z^2}" orbitals actually contain some contributions of 6s and 6p orbitals, but for simplicity are designated as

such.

27 The reverse reaction, reaction of **6** with an excess of $cdoH_2$, afforded hardly **3**. The reason is not clear.

28 T. Yamaguchi, Ph. D Thesis, Tohoku University (1990).

29 N. Walker and D. Stuart, *Acta Crystallogr., Sect. A*, **A39**, 158 (1983).

30 P. T. Beurskens, G. Admiraal, W. P. Bosman, S. Garcia-Granda, R. O. Gould, J. M. M. Smits, and C. Smykalla, "The DIRDIF program system," (1992).

31 "teXsan, single crystal structure analysis software, version 1.7," Molecular Structure Corporation, The Woodlands, TX (1995).

32 L. Vassidei and Q. Sciacovelli, *QCPE*, No. **458**.